

# Sonochemical Synthesis of Well-Dispersed Gold Nanoparticles at the Ice Temperature

Chia-Hao Su, Pei-Lin Wu,\* and Chen-Sheng Yeh\*

Department of Chemistry, National Cheng Kung University, Tainan 701, Taiwan, ROC

Received: May 26, 2003; In Final Form: August 27, 2003

A newly modified sonochemical approach was demonstrated to synthesize stable Au suspensions. The formation of Au nanoparticles with diameters of  $\sim 20$  nm was accomplished through the ultrasonic irradiation of aqueous  $\text{HAuCl}_4$  solutions containing trisodium citrate at  $4^\circ\text{C}$ . The efficient generation in gold particles only occurred when the sufficient citrate concentrations (1.9, 2.9, and 3.9 mM) were reached. At low citrate concentrations ranging from 0.49 to 1.5 mM, large aggregates of coalesced Au particles were observed as sonication time increased. It is proposed that citrate could transform as the reducing radicals, 1,2,3-tricarboxy-2-propyl radicals, for the  $\text{AuCl}_4^-$  reduction and might also act as the stabilizer during particles formation.

## Introduction

Various nanosized colloids have attracted considerable interest as they exhibit conspicuous physicochemical properties. Among the variety of the metal nanometer particles, Au is the most well studied and has been widely applied to various applications such as catalysis, biological reporters, electronic and optic materials.<sup>1–6</sup> Continuous effort in developing preparation strategy is always an important requisite for the fabrication of advanced integrated functionalized-materials based on the nanoparticles.

There are many established methods for synthesizing metal nanoparticles, including conventional,<sup>7</sup> sonochemical,<sup>8</sup> photolytical,<sup>9</sup> and radiolytic reduction.<sup>10</sup> A survey of the synthetic reports clearly indicates that nanoparticle properties, such as stability and particle sizes, strongly rely on the experimental methodology and the employed conditions. It is well-known that ultrasonic irradiation of water molecules leads to the formation, expansion, and collapse of the cavitation bubbles in the irradiated aqueous solution.<sup>8,11</sup> Following the process of the bubbles imploding, the interior water vapor is dissociated into H atoms and OH radicals. The resulting radicals initiating sequential abstraction and reduction reactions have been used to generate various metallic colloids. As a result, the sonochemical method provides an attractive route to prepare metal nanoparticles, e.g., Au,<sup>8a–g</sup> Ag,<sup>8h</sup> CdS.<sup>8j</sup>

Sonochemical reduction often used alcohols, e.g., 2-propanol, or surfactants, e.g., sodium dodecyl sulfate or both (alcohol/surfactant) as radical scavenging solutes for the subsequent colloidal formation. Sometimes, an additional polymer was added as the stabilizer.<sup>8</sup> It is worth noting that there are only some sonochemical reports on the formation of the Au nanoparticles,<sup>8a–g</sup> although Au particles have been extensively investigated in many aspects. In all previous Au ultrasonic works, the common tactics have been using alcohols and/or surfactants to facilitate  $\text{AuCl}_4^-$  reduction. Furthermore, the surfactants or polymers were used to provide effective protection for stable Au suspensions.<sup>8a–c,g</sup>

In the present studies, a newly modified sonochemical strategy was developed to initiate  $\text{AuCl}_4^-$  reduction without addition of

alcohols and surfactants. The well-dispersed Au nanoparticles were prepared in the presence of trisodium citrate under the ice condition ( $\sim 4^\circ\text{C}$ ). The particle sizes and efficiency of Au formation are highly dependent on the concentrations of trisodium citrate in aqueous solutions.

## Experimental Section

All solutions were prepared using Milli-Q water.  $\text{HAuCl}_4 \cdot 3\text{H}_2\text{O}$  was obtained from Alfa Aesar Chemical Co. and trisodium citrate ( $\text{C}_6\text{H}_5\text{Na}_3\text{O}_7$ ) (99.0%) was purchased from Showa Chemical Co.

An aqueous solution of  $\text{HAuCl}_4$  (5 mM, 0.5 mL) was added to 4.5 mL of distilled water in a sonication vessel, followed by mixing with different concentrations of trisodium citrate. Ultrasonic irradiation was performed using an ultrasonic generator (Sonicator, XL2020, 20 kHz) with a 3.2 mm diameter of barium titanate oscillator to deliver a 110 W power. The sonication was operated at continuous irradiation under aerobic condition. During the irradiation the sample vessels were maintained in an ice bath ( $\sim 4^\circ\text{C}$ ).

The sonication was stopped at various time periods for the recording of UV–vis spectra and the sample preparation of TEM images. A UV–vis spectrophotometer was used to measure the resulting Au solutions. Electron micrography was performed using a transmission electron microscope (JEOL JEM-1200 EX). The average diameter and size distribution were calculated using Sigma Scan Pro 5.0 software for image analysis.

## Results and Discussion

In this study, trisodium citrate was added in a solution of  $\text{HAuCl}_4$  for sonication. The changes in the concentrations of trisodium citrate were conducted to achieve the optimal conditions for Au colloidal formation. We performed a series of concentrations, 0.49, 0.97, 1.5, 1.9, 2.9, and 3.9 mM, corresponding to molar ratios of  $\text{HAuCl}_4:\text{C}_6\text{H}_5\text{Na}_3\text{O}_7$  with 1:1, 1:2, 1:3, 1:4, 1:6, and 1:8, respectively. It is interesting that two distinctly differential behaviors of UV–vis absorption upon ultrasonic irradiation were observed between lower amounts (0.49, 0.97, 1.5 mM) and relatively higher concentration regimes (1.9, 2.9, 3.9 mM) of trisodium citrate. The sample containing 0.97 mM trisodium citrate (Figure 1) was presented to show

\* To whom correspondence should be addressed. E-mail: wupl@mail.ncku.edu.tw; csyeh@mail.ncku.edu.tw.

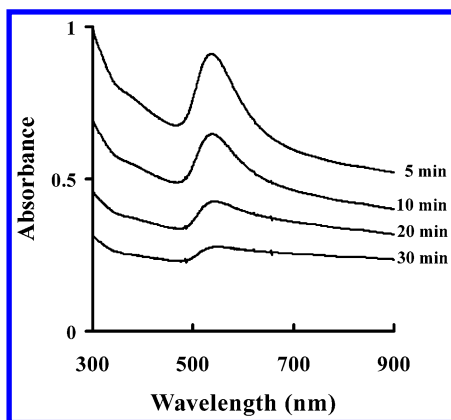


**Figure 1.** Optical absorption measured as a function of irradiation time at 0.97 mM citrate.

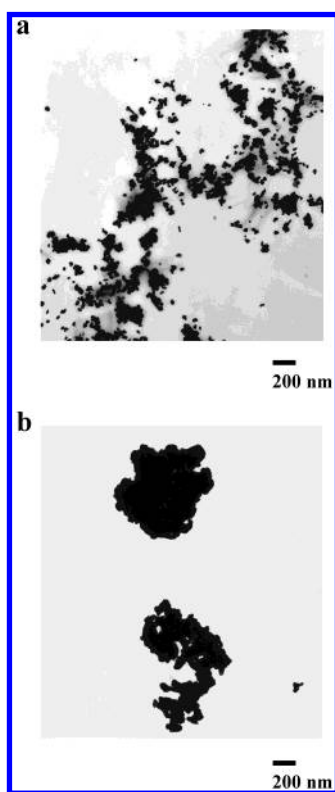


**Figure 2.** TEM images of Au nanoparticles prepared at 0.97 mM citrate after sonication for (a) 10 min and (b) 20 min.

the typical alterations in the UV–vis absorbance varied with sonication time. Upon the early ultrasonic irradiation, the solutions were transformed from the initial yellow to a purple color. An absorption maximum at 539 nm, attributed to a Au plasmon band, was observed at 5 min sonication. As the sonication times prolonged, the evolution in the absorption spectra showed a continuous descent in magnitude, accompanied by a coloring conversion into transparency for solutions. Figure 2 exhibits the corresponding TEM images taken at 10 and 20 min. In the early irradiation stage, many small particles were generated and seriously aggregated as irregular islands (Figure 2a). However, the particles coalesced together, forming large aggregates as the irradiation period extended to 20 min (Figure 2b). In fact, the Au colloids eventually settled out of the solutions. TEM results clearly explicate the decreased behavior in the UV–vis absorbance with longer sonication time.

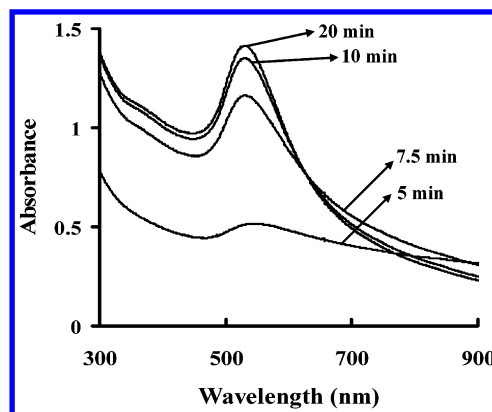


**Figure 3.** Optical absorption measured as a function of irradiation time at 3.9 mM citrate.

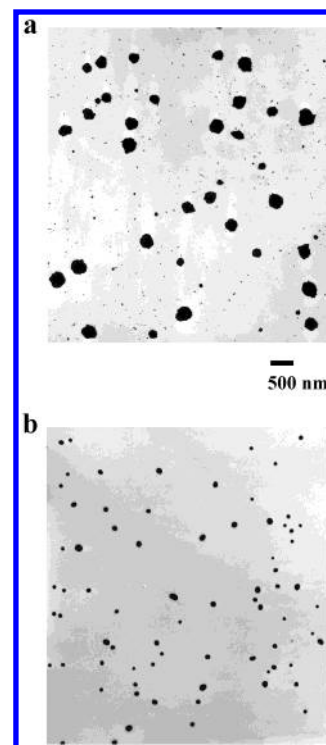


**Figure 4.** TEM images of Au nanoparticles prepared at 3.9 mM citrate after sonication for (a) 2.5 min and (b) 25 min.

Conversely, the opposite profile in the absorption spectra of the colloidal solutions was observed when higher  $\text{C}_6\text{H}_5\text{Na}_3\text{O}_7$  concentrations (1.9, 2.9, and 3.9 mM) were used, where the Au characteristic peak gradually enhanced as the duration of the sonication increased until the  $\text{AuCl}_4^-$  was reduced completely at approximate 20–30 min. The resulting colloidal solutions stayed a purplish color and remained stable for at least 3 months. Figure 3 presents the optical absorption of the suspensions containing 3.9 mM trisodium citrate. The Au plasmon band exhibited a blue shift (528 nm) as compared with the sets of the solutions with lower  $\text{C}_6\text{H}_5\text{Na}_3\text{O}_7$  concentrations. Figure 4a,b represents the TEM micrograph captured after 2.5 and 25 min reaction periods, respectively. Initially, the large colloidal lumps incorporating with relatively small and spherical-like particles coexisted in the solutions. As the irradiation lengthened, the suspensions appeared as well-separated and spherical morphology. It seems that sonication induces the

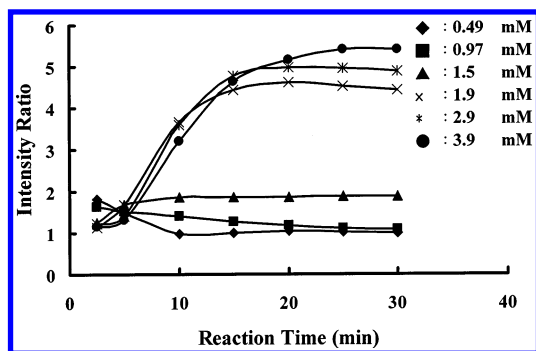


**Figure 5.** Development of the Au colloidal formation as a function of sonication time under various citrate concentrations. The intensity ratios were calculated from the intensities of the Au surface plasmon bands (528 or 539 nm) and the position at 700 nm (arbitrarily selected).

**TABLE 1: Average Particle Diameters (nm) of Gold Particles Attained on Sonication of  $\text{AuCl}_4^-$  in the Presence of Different Citrate Concentrations under Various Irradiation Times**

concn of citrate (mM)	irradiation time (min)			
	15	20	25	30
1.9	$19.4 \pm 1.8$	$19.8 \pm 1.8$	$18.9 \pm 1.1$	$18.9 \pm 1.4$
2.9	$18.2 \pm 1.5$	$20.6 \pm 2.1$	$20.6 \pm 0.3$	$20.9 \pm 1.1$
3.9	$16.9 \pm 1.5$	$20.9 \pm 0.9$	$21.2 \pm 0.9$	$22.0 \pm 0.8$

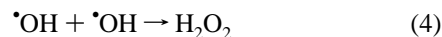
disintegration process of the large-sized particles into smaller ones.

For comparison, the spectral intensity versus sonication time was monitored at various trisodium citrate concentrations, as shown in Figure 5. The spectral intensities were obtained by evaluating the intensity ratios between Au surface plasmon positions (539 or 528 nm) and the absorbance at 700 nm (arbitrarily chosen). Two sets of distinct profiles were clearly obtained. At higher citrate concentrations (1.9, 2.9, and 3.9 mM), the intensity of the absorbance behaved with an ascending trend until reaching the limiting time ( $\sim 20$  min), indicating the complete growth of the Au nanoparticles. On the other hand, the intensity development becomes much less prominent when citrate concentrations were reduced. Figure 5 demonstrates that gold colloidal formation strongly relied on the citrate concentrations and the progress of the gold(III) reduction changed during the ultrasonic irradiation. Particle sizes were calculated at irradiation times of 15, 20, 25, and 30 min for 1.9, 2.9, and 3.9 mM citrate concentrations and are summarized in Table 1. The particle diameters remained constant after 20 min of sonication in each given citrate dosage, attributed to the termination of the  $\text{AuCl}_4^-$  reduction. Au particles exhibited slight growth in sizes,  $19 \rightarrow 20 \rightarrow 21$  nm, as the citrate concentrations increased from 1.9 to 3.9 mM.

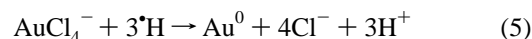
The aforementioned sonochemical results were conducted at  $\sim 4^\circ\text{C}$ . Two additional experiments using no sonolysis at the ice temperature and with sonication at room temperature were performed to elucidate the distinction. Without sonication by simply mixing  $\text{HAuCl}_4$  and  $\text{C}_6\text{H}_5\text{Na}_3\text{O}_7$  at  $4^\circ\text{C}$ , either 0.49 or 3.9 mM of trisodium citrate dosages did not induce reaction and the solutions retained the original light yellow color, showing no Au plasmon absorption even after a reaction period of 1 h. When the sonication was operated at room temperature ( $24\text{--}25^\circ\text{C}$ ), the differential particles formation was observed as compared with the results described at  $4^\circ\text{C}$ . Following the graphics in Figure 5, the spectral intensity ratios were plotted as a function of sonication time. The profile showed that the intensity of the absorbance gradually developed to a maximum,

subsequently turned into descent for citrate concentrations at 1.9, 2.9, and 3.9 mM (see figure in Supporting Information). It was observed that the particles were mainly formed as coagulation domains at 15 min sonolysis (near the maximum intensity ratio) whereas the isolated Au colloids accompanied with aggregatemorphology were attained as the irradiation extended to 30 min. In addition, the prepared Au diameters showed broad distributions and no dependence of citrate dosages in particle sizes (see TEM and calculated diameters in Supporting Information). On the other hand, the same progress as observed at the ice temperature exhibited no apparent intensity development at low citrate concentrations. Based on the above studies, this seems to indicate that the low temperature ( $\sim 4^\circ\text{C}$ ) provided a mild circumstance to form the well-dispersed Au suspension.

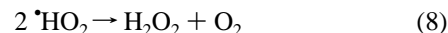
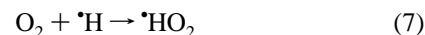
It has been well documented that sonication irradiates  $\text{H}_2\text{O}$ , which generates  $\text{H}^\bullet$  and  $\text{OH}^\bullet$  to further initiate the process of the sonochemical reduction.<sup>8</sup> Water sonolysis could induce the following reaction sequences:



Our ultrasonic conditions differed from previously reported strategies in that the presence of the organic compounds, i.e., the alcohols and surfactants, could act as the radical scavengers in the subsequent reduction. Here, it is proposed that the primary reducing radical  $\text{H}^\bullet$  (reaction 1) triggered the reduction of  $\text{AuCl}_4^-$ , followed by the condensation for the Au colloidal growth (reactions 5 and 6). However, the studies on the



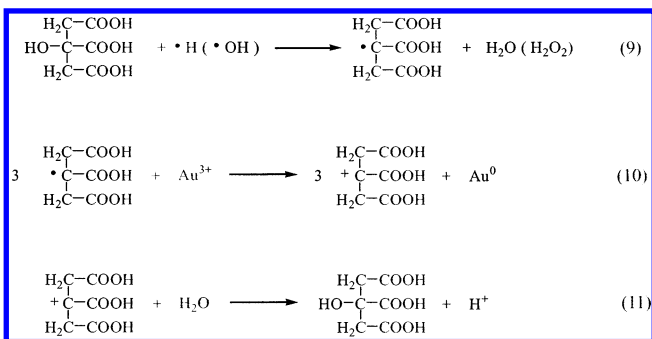
formation rate of the gold particles in the sonolysis under air from Nagata and co-workers is worth mentioning.<sup>8c</sup> In the presence of an oxygen atmosphere,  $\text{H}^\bullet$  would combine with  $\text{O}_2$ , leading to  $\text{HO}_2^\bullet$  formation, as shown in reactions 7 and 8.



Therefore, reaction 7 provides an additional pathway in competition with the  $\text{AuCl}_4^-$  reduction (reaction 5). Further experiments pertaining to the effect of atmospheric gases should be performed in an anaerobic environment for detailed Au formation mechanisms.

On the basis of the previous studies, the organic compounds acting as scavengers reacted with the primary radicals, giving rise to the secondary radicals.<sup>8</sup> A parallel experiment was performed by sonochemical reduction of  $\text{AuCl}_4^-$  without addition of citrate. The resulting solutions stayed as transparency and showed no signal of the UV-vis absorbance after sonication for 40 min, indicating the absence of the Au particles. On the basis of the aforementioned results, citrate should contribute to the reduction of the  $\text{Au}^{3+}$  ions. We have measured the mixtures ( $\text{HAuCl}_4$  + sodium citrate) before performing sonication and

the supernatant solutions collected from the resulting suspensions after irradiation for NMR analysis. Both  $^1\text{H}$  NMR measurements showed evidence for the presence of the citric acid. Therefore, we assume that the reactions proceeded as follows.



Due to the addition of the citrate in our experiments, 1,2,3-tricarboxy-2-propyl radicals acted as the reducing radicals via  $\cdot\text{H}(\cdot\text{OH})$  abstraction and possibly resulted in the reduction of gold ions (reactions 9–11). Following the reaction 11 in aqueous solution would lead to the resulting product, citric acid.

Although the reaction processes involving in 1,2,3-tricarboxy-2-propyl radicals are not clarified yet, reactions 9–11 reasonably describe the observation of both Au particles and citric acid in suspensions. As shown earlier, a bizarre behavior occurred for the formation of some large chunky colloids at the very early stage (Figure 4a). There is no such observation at low citrate concentrations. This could be interpreted as the generation of significant amounts of the  $\text{Au}^0$  nuclei, due to the presence of sufficient citric acid at higher concentrations. Subsequently, the  $\text{Au}^0$  quickly condensed and grew into large colloids. However, the underlying mechanisms remain to be unraveled.

Finally, although citrate formed as citric acid for the subsequent reduction reactions, the existence of the citrate acting as protection agent could not be excluded completely. For example, there was not sufficient citrate to build up the protection layer around the Au particle at low citrate concentrations, leading to significant aggregation at early irradiation (Figure 2a). Because the insufficiently stabilized Au particles were produced, the coalescence took place to form large structures (Figure 2b). In the presence of higher citrate concentrations, it could be appreciated that completely citrate-stabilized Au particles prevented further coalescence and resulted in the well-separated gold suspensions.

## Conclusion

Without alcohols and stabilizers, e.g., surfactants and polymers, the dispersed Au nanoparticles were prepared using

ultrasound irradiation methodology. From both UV–vis and TEM studies, the citrate dosages gave a drastic effect on the formation of the gold particles. Only sufficient citrate concentrations (1.9, 2.9, and 3.9 mM) resulted in well-separated Au particles with the diameters of  $\sim 20$  nm. The addition of citrate to yield Au suspension was suggested to provide two functionalities: initiating reduction and protection. Although we have described a newly preparative strategy in sonolysis, it is inspiring to engage in further examination of the detailed mechanisms involving the radical scavengers and the scavenging process.

**Acknowledgment.** We thank the National Science Council of the Republic of China for its financial support for this work. We also acknowledge Ms. S. Y. Hsu for the TEM measurements at Tainan Regional Instrument Center, National Cheng Kung University.

**Supporting Information Available:** Table of room temperature particle diameters, profile of Au colloidal formation as a function of sonication time, and TEM images of Au nanoparticles. This material is available free of charge via the Internet at <http://pubs.acs.org>.

## References and Notes

- Henglein, A. *J. Phys. Chem.* **1980**, *84*, 3461.
- Majetich, A.; Artman, J. O.; McHenry, M. E.; Nuhfer, N. T.; Staley, S. W. *Phys. Rev. B* **1993**, *48*, 16845.
- Storhoff, J. J.; Elghanian, R.; Mucic, R. C.; Mirkin, C. A.; Leister, R. L. *J. Am. Chem. Soc.* **1998**, *120*, 1959.
- Li, Y.; Hong, X. M.; Collard, D. M.; El-Sayed, M. A. *Org. Lett.* **2000**, *2*, 2385.
- Feldheim, D. L.; Keating, C. D. *Chem. Soc. Rev.* **1998**, *27*, 1.
- Mukhopadhyay, K.; Phadtare, S.; Vinod, V. P.; Kumar, A.; Rao, M.; Chaudhari, R. V.; Sastry, M. *Langmuir* **2003**, *19*, 3858.
- Ahmadi, T. S.; Wang, Z. L.; Green, T. C.; Henglein, A.; El-Sayed, M. A. *Science* **1996**, *272*, 1924.
- See for example: (a) Yeung, S. A.; Hobson, R.; Biggs, S.; Grieser, F. *J. Chem. Soc., Chem. Commun.* **1993**, 378. (b) Okitsu, K.; Mizukoshi, Y.; Bandow, H.; Maeda, Y.; Yamamoto, T.; Nagata, Y. *Ultrason. Sonochem.* **1996**, *3*, S249. (c) Nagata, Y.; Mizukoshi, Y.; Okitsu, K.; Maeda, Y. *Radiat. Res.* **1996**, *146*, 333. (d) Grieser, F.; Hobson, R.; Sostaric, J.; Mulvaney, P. *Ultrasonics* **1996**, *34*, 547. (e) Okitsu, K.; Yue, A.; Tanabe, S.; Matsumoto, H.; Yobiko, Y. *Langmuir* **2001**, *17*, 7717. (f) Okitsu, K.; Yue, A.; Tanabe, S.; Matsumoto, H.; Yobiko, Y.; Yoo, Y. *Bull. Chem. Soc. Jpn.* **2002**, *75*, 2289. (g) Caruso, R. A.; Ashokkumar, M.; Grieser, F. *Langmuir* **2002**, *18*, 7831. (h) Pol, V. G.; Srivastava, D. N.; Palchik, O.; Palchik, V.; Slifkin, M. A.; Weiss, A. M.; Gedanken, A. *Langmuir* **2002**, *18*, 3352. (i) Aurbach, D.; Nimberger, A.; Markovsky, B.; Levi, E.; Sominiski, E.; Gedanken, A. *Chem. Mater.* **2002**, *14*, 4155. (j) Mastai, Y.; Polsky, R.; Koltypin, Y.; Gedanken, A.; Hodes, G. *J. Am. Chem. Soc.* **1999**, *121*, 10047.
- Ohtaki, M.; Tushima, N. *Chem. Lett.* **1990**, 489.
- Gutiérrez, M.; Henglein, A. *J. Phys. Chem.* **1993**, *97*, 11368.
- Suslick, K. S.; Hammerton, D. A.; Cline, R. E. *J. Am. Chem. Soc.* **1986**, *108*, 5641.